Fluorescent Sensors For Hg^{2+} and Cu^{2+} Based On Condensation Products of 4H-1,2,4 Triazole-4-Amine And Carboxylated Benzoic Acids

Satyapriya Deka
Gauhati University
Ankur K Guha
Cotton University
Diganta Kumar Das (digkdas@yahoo.com)
Gauhati University https://orcid.org/0000-0001-5507-016X

Research Article

Keywords: Copper, Benzoic acid, Phthalic acid, Sensor, Fluorescence, DFT

Posted Date: May 11th, 2021

DOI: https://doi.org/10.21203/rs.3.rs-400901/v1

Abstract

Mercury (Hg) causes serious health issues in its all forms. Deficiency as well as excess of copper ion (Cu^{2+}) in human body is hazardous. A series of four compounds have been derived from carboxylated benzoic acids (benzoic acid, isophthalic acid, terephthalic acid and phthalic acid) and 4H-1,2,4 triazole-4-amine and characterized. Fluorescencce detection of Hg^{2+} was recorded by the derivates with benzoic acid and isophthalic acid while the derivatives of terephthalic acid and phthalic acid detect Cu^{2+} by fluorescence “off” mode. Metal ions like Li^{+}, Na^{+}, K^{+}, Zn^{2+}, Al^{3+}, Mg^{2+}, Mn^{2+}, Co^{2+}, Ni^{2+}, Cu^{2+}, Cd^{2+}, Pb^{2+} and Hg^{2+} found not to interfere. The stoichiometry of binding is 1:1 for the benzoic acid derivative with Hg^{2+} while it is 1:2 for the other three derivatives. The binding constants are *ca.* $10^{-4.5}$ between the sensors and Hg^{2+} or Cu^{2+} and detection limits are around $10^{-5.5}$ M. DFT calculation provided optimized geometries of the sensors and confirmed the stoichiometry of binding with Hg^{2+}/Cu^{2+}.

Introduction

Most of the heavy metals in ionic form are hazardous to the environment and human health and one of them is Mercury ion (Hg^{2+}) [1]. The relatively high stability of Hg^{2+} ion enable it to reach human body through water, soil, air and food chain [2]. Hg^{2+} ions severely affect many living organisms [3]. Power plants release considerable amount of Hg^{2+} into the atmosphere due to burning of large quantity of coal and hence releasing Hg^{2+} [4]. Batteries, pesticides and paper mills are other major sources of Hg^{2+} pollution. Compact Fluorescent Lamps contain Hg^{2+} ions and have become a matter of great environmental concern as unscientific disposal of CFLs acts as source of Hg^{2+} pollution [5]. Hg^{2+} is more toxic in metalo-organic form and can lead to deterioration of brain, hamper fetus growth [6], can damage immune system, kidney, heart, and lung of human being [7]. Hence monitoring system for Hg^{2+} in water has been a matter of utmost importance with respect to the environmental and human health.

The common strategy for developing sensor for Hg^{2+} is to synthesize molecules containing S so as to form Hg-S bonds which leads to structural change observed spectroscopically or reaction giving new spectroscopically active molecules (chemodosimeters) [8–13]. The occurance of mercury in sulfur rich environment is a disadvantage of S based fluorescent sensors for Hg^{2+} [14]. Direct chelation of S based molecules to Hg^{2+} and subsequent fluorescence enhancement are not known much [15–17]. Schiff bases, due to easy synthetic procedure, have gained interest as sensor for metal ions. The number of Schiff’s bases not having S but act as Hg^{2+} fluorescence sensor are rare. Examples can be cited are Schiff base obtained from - α-naphthaldehyde with naphthylamine [18], N-phenylthiosemicarbazide and 2-naphthaldehyde [19] etc. Amide armed calix[4]-aza-crown based sensor containing S is reported but Hg^{2+} binds to N atoms [20], sensor based on a pentaaza macrocycle conjugated to a hemicyanine dye where Hg^{2+} binds to carboxylate is known [21]. Hence development of fluorescence sensor for Hg^{2+} without having S must be of interest.

Copper is the third most abundant metal in the globe. It is involved in many critical life processes like – photosynthesis, respiration, superoxide dismutase etc. Excess accumulation of Cu^{2+} in human body may cause severe health problems like Parkinson's, Alzheimer's, Menke's and Wilson's disease [22–25]. Retarded growth and defective nervous system is related to deficiency of copper [26]. Industries like electroplating, electric gadgets, alloy etc are the sources of major copper pollutions. Therefore development of simple but sensitive methods to detect Cu^{2+} is of great importance. Schiff bases which are simple to synthesis and highly sensitive as fluorescent sensor for Cu^{2+} are known [27, 28].

In this paper we report the synthesis and characterization of a series of four compounds derived from 4H-1,2,4 triazole-4-amine and carboxylated benzoic acids. The two compounds obtained from 4H-1,2,4 triazole-4-amine with benzoic acid and isophthalic acid act as fluorescent sensor for Hg^{2+} while the other two compounds obtained from 4H-1,2,4 triazole-4-amine with phthalic acid and terephthalic acid are found to act as fluorescent sensor for Cu^{2+} based on fluorescent quenching. DFT structure optimization of the sensors as well as their Hg^{2+}/Cu^{2+} complexes reported and found to be in conformity to experimental results.

Experimental

Materials and methods

The chemicals have been procured either from Sigma Aldrich or LOBA Chemie. Except for $Pb(NO_3)_2$, $CdCl_2$ and $HgCl_2$ the other metal salts are sulfates. Double distilled water obtained from quartz double distillation plant were used to prepare metal salt solutions (0.01M). The FT-IR spectra were recorded as KBr pallet in Perkin Elmer RXI spectrometer. NMR spectra (^1H and ^{13}C) were obtained using Bruker Ultra Shield 300 MHz spectrophotometer using $CDCl_3$ or DMSO-d_6 as solvent. The UV/Visible spectra were recorded in Shimadzu UV 1800, fluorescence in HITACHI 2700 and HRMS in WATERS Q-TOF premier mass spectrometer.

Synthesis and characterization of AM1

Benzoic acid (0.1 g, 0.818 mmol) was taken in DCM (10 mL), cooled in an ice bath and EDC.HCl (3-(Ethylamine) methylene) amino)-*N*, *N*-dimethylpropan-1-amine hydrochloride) (0.188 g, 0.982 mmol) was added followed by DMAP (*N*, *N*-dimethyl amino pyridine-4-amine) (0.025 g, 0.163 mmol). After 10 minutes, 4*H*-1,2,4-triazole-4-amine (0.068 g, 0.818 mmol) was added and allowed to stir at room temperature for 10 h. After completion of the reaction, the reaction mixture was washed twice with brine (20 mL), 2N HCl (20 mL), saturated $NaHCO_3$ (20 mL). The organic layer was dried over anhydrous Na_2SO_4 and evaporated to get the product. White solid. Yield 77%, m.p. 238°C.

^1H NMR (300 MHz, $CDCl_3$): δ = 8.25 (s, 1H), 7.97 (d, *J* = 8.4 Hz, 2H), 7.45 (d, *J* = 8.5 Hz, 2H), 7.35 (t, *J* = 7.4 Hz, 5H), 7.27 (s, 1H).

^{13}C NMR (75 MHz, DMSO): δ = 167.59, 144.06, 132.80, 131.11, 129.37, 128.87, 127.85.

HRMS (ESI-TOF): m/z: $[M + H]^+$ calculated for $C_9H_9N_4O$ 189.0776, found: 189.0776

Synthesis and characterization of AM2

Isophthalic acid (0.2g, 1.2 mmol) was taken in DMF (5 mL), cooled in an ice bath and EDC.HCl (0.276g, 1.44 mmol) was added followed by DMAP (0.014g, 0.120 mmol). After 10 minutes, 4*H*-1,2,4-triazole-4-amine (0.202g, 2.40 mmol) was added and allowed to stir at room temperature for 10 hours. After completion of the reaction, reaction mixture was extracted with ethyl acetate and washed twice with brine (20 mL), 2N HCl (20 mL), saturated $NaHCO_3$ (20 mL). The organic layer was dried over anhydrous Na_2SO_4 and evaporated to get the desired product. White solid. Yield 66%.

^{1}H NMR (300 MHz, $CDCl_3$): δ = 8.39 (s, 2H), 7.92 (d, *J* = 7.7 Hz, 5H), 7.31–7.21 (m, 3H)

^{13}C NMR (75 MHz, $CDCl_3$): δ = 166.98, 132.95, 132.68, 130.43, 130.23, 127.71

HRMS (ESI-TOF): m/z: $[M + H]^+$ calculated for $C_{12}H_{11}N_8O_2$ is 299.1005, found: 299.1000

Synthesis and characterization of AM3

Terephthalic acid (0.2g, 1.2 mmol) was taken in DMF (5mL), cooled in an ice bath and EDC.HCl (0.276g, 1.44 mmol) was added followed by DMAP (0.014g, 0.120 mmol). After 10 minutes, 4*H*-1,2,4-triazole-4-amine (0.202g, 2.40 mmol) was added and allowed to stir at room temperature for 10 h. After completion of the reaction, reaction mixture was extracted with ethyl acetate and washed twice each with brine (20 mL), 2N HCl (20 mL), saturated $NaHCO_3$ (20 mL). The organic layer was dried over anhydrous Na_2SO_4 and evaporated to get the desired product. White solid. Yield 58%.

^{1}H NMR (300 MHz, DMSO): δ = 8.38 (s, 1H), 8.01 (s, 9H).

^{13}C NMR (75 MHz, DMSO): δ = 166.93, 134.75, 129.55.

HRMS (ESI-TOF): m/z: $[M + Na]^+$calculatedd for $C_{12}H_{10}N_8NaO_2$322.0858, found: 322.1777

Synthesis and characterization of AM4

Phthalic acid (0.2g, 1.2 mmol) in DMF (5 mL) + EDC.HCl (0.276 g, 1.44 mmol) + DMAP, 4*H*-1,2,4-triazole-4-amine (0.202 g, 2.40 mmol) (after 10 minutes), stirred at room temperature for 10 h,. After completion of the reaction, the reaction product was extracted with ethyl acetate and washed twice each with brine (20 mL), 2N HCl (20 mL), saturated $NaHCO_3$ (20 mL). The organic layer was dried over anhydrous Na_2SO_4 and evaporated to get the desired product. White solid. Yield 66%.

IR (KBr): 3455 cm^{-1}, 1635 cm^{-1}, 1561 cm^{-1}, 1413 cm^{-1}.

^{1}H NMR (300 MHz, DMSO-D_6): δ8.46 (s, 2H), 8.04 (d, *J* = 7.3, 1H), 7.95 (s, 2H), 7.70–7.53 (m, 5H)

HRMS (ESI-TOF): m/z: $[M + Na]^+$ calculatedd for $C_{12}H_{10}N_8NaO_2$: 322.0858, found: 322.1791.

Computational Details

All the structures were fully optimized at M06-2X/6-311 + + G** level of theory without any symmetry constraints [29]. At the same level of theory frequency calculations were performed to understand the nature of the stationary states. All these structures were found to be local minima with all real frequencies. Effective core potential basis set of Stuttgart/Dresden (SDD) were used for Hg atom. Natural bond orbital analyses (NBO) [30] were performed to understand the electronic feature of these systems. All these calculations were performed using Gaussian16 suite of program [31].

Results And Discussion

Effect of different metal ions on fluorescence spectra of AM1, AM2, AM3 and AM4

Fluorescence spectra of AM1 (5×10^{-6} M, CH_3CN), AM2 (5×10^{-6} M, CH_3CN), AM3 (5×10^{-6} M, CH_3OH) and AM4 (5×10^{-6} M, 1:1 *v/v* CH_3:H_2O) were recorded with excitation wave length 250 nm for AM1 and AM2, while 270 nm for AM3 and AM4. Emission peaks were observed (with their intensity mentioned within bracket) for AM1, AM2, AM3 and AM4 respectively at 303 nm (241 a.u), 310 nm (430 a.u), 310 nm (251 a.u) and 310 nm (204 a.u).

The solutions of AM1, AM2, AM3 and AM4 were titrated with the metal ions - Li^+, Na^+, K^+, Mg^{2+}, Mn^{2+}, Co^{2+}, Ni^{2+}, Cu^{2+}, Zn^{2+}, Cd^{2+}, Al^{3+}, Pb^{2+} and Hg^{2+}. The fluorescence intensity of AM1 and AM2 were quenched by Hg^{2+} while other metal ions did not affect the fluorescence intensity significantly. In case of AM3 and AM4 the fluorescence intensity was found to be quenched by Cu^{2+} while other metal ions had no significant affect. Figure 1A and Fig. 1B show the effect of increasing concentration of Hg^{2+} on fluorescence intensity quenching of AM1 and AM2 respectively. Figure 1C and Fig. 1D show the gradual quenching effect of Cu^{2+} concentration on fluorescence intensity of AM3 and AM4 respectively.

Selectivity and interference studies

Figure 2A to Fig. 2D compares the I_0/I values of AM1, AM2, AM3 and AM4 through bar diagrams in presence of one equivalent of Hg^{2+} in case of AM1, AM2 and one equivalent of Cu^{2+} in case of AM3, AM4. Here I_0 is the fluorescence intensity of AM1, AM2, AM3 and AM4 in absence of Hg^{2+} or Cu^{2+}. I is the fluorescence intensity in presence of one equivalent of Hg^{2+} or Cu^{2+}. From the figure it is clear that the height of the bar corresponding to Hg^{2+} is quite distinct for AM1 and AM2 compared to other metal ions while the height of the bar corresponding to Cu^{2+} is distinct for AM3 and AM4 compared to other metal ions.

The interference possibilities of other metal ions on the sensing abilities of AM1 to AM4 towards Hg^{2+} or Cu^{2+} were studied. For this purpose one equivalent of a metal ion was added into the solution of AMX (X = 1–4) and allowed to equilibrate for 5 minutes. Then one equivalent of Hg^{2+} (for X = 1,2) or Cu^{2+} (for X = 3,4) was added and again allowed to equilibrate for about 5 minutes. The fluorescence spectrum was then recorded. It was observed that Hg^{2+} or Cu^{2+} could quench the fluorescence intensity of the respective sensor solution even in presence of another metal ion to the same extent when Hg^{2+} or Cu^{2+} was added to the sensor solution in absence of the other metal ion. This has been illustrated in Fig. 3(A to D) through bar diagrams.

Determination of binding constants and stoichiometry of binding

The binding constants and the stoichiometry of binding between the sensors (AM1 to AM4) and Hg^{2+} or Cu^{2+} were determined from the fluorescence titration data of the sensor against Hg^{2+} or Cu^{2+}. The $\log[(I_0-I_s)/(I_s-I_f)]$ was plotted versus log of the concentration of Hg^{2+} or Cu^{2+}. The binding constant and the stoichiometry of binding were obtained as reported [32]. Here, I_0 is the fluorescence intensity of AM1 and AM2 or AM3 and AM4 prior to addition of Hg^{2+} or Cu^{2+} respectively, I_s is the fluorescence intensity of AM1 and AM2 or AM3 and AM4 at an intermediate added concentration of Hg^{2+} or Cu^{2+} respectively, I_f is the fluorescence intensity of AM1 and AM2 or AM3 and AM4 in presence of one equivalent of Hg^{2+} or Cu^{2+} respectively. The binding constant was found to be $10^{4.3}$ for AM1 towards Hg^{2+} with 1:1 binding ratio; for AM2 towards Hg^{2+} it was calculated as $10^{4.2}$; the binding constant for AM3 and Cu^{2+} system is $10^{4.5}$ while the binding constant was calculated as $10^{4.1}$ M for AM4 and Cu^{2+} system. In case of the three sensors L2 to L4 the sensor:metal ratio was found to be 1:2.

The sensor AM1 has been synthesized from monocarboxylic derivative of benzene while the sensors AM2, AM3 and AM4 were synthesized from dicarboxylic derivatives of benzene by reacting with 4*H*-1,2,4-triazole-4-amine. Hence AM1 has one NNO binding sites while the others i.e. AM2, AM3 and AM4 have two NNO binding sites each. Therefore the binding ratio of sensor to metal is 1:1 in case of AM1 while it is 1:2 in case of the other three sensors. The fluorescence quenching of sensors due to interaction with Hg^{2+} or Cu^{2+} is due to decrease in conjugation upon binding.

UV/Visible spectral analysis of sensor and metal ion interactions

UV/Visible spectral titrations were done for the sensors AM1 and AM2 with Hg^{2+} and for AM3 and AM4 with Cu^{2+}. Figure 4A and 4B shows the UV-Visible spectral changes of AM1 and AM2 at different added concentrations of Hg^{2+} while Fig. 4C and Fig. 4D shows UV-Visible spectral changes of AM3 and AM4 at different added concentration of Cu^{2+}. From the figures it is clear that the effect of Hg^{2+} on the spectrum of AM1 is not significant (Fig. 4A). AM2 shows a shoulder at 250 nm and upon addition of Hg^{2+} the shoulder gradually becomes a well defined peak at 230 nm (Fig. 4B). AM3 shows a peak at 280 nm and with the addition of Cu^{2+} the absorbance decreases without any change in peak position (Fig. 4C). AM4

shows one peak at 260 nm which on gradual addition of Cu^{2+} decreases its absorbance with a shift in peak position to 240 nm (Fig. 4D). AM1 binds to one Hg^{2+} while the other three sensors bind to two of either Hg^{2+} or Cu^{2+} (Scheme 2). Hence the effect of Hg^{2+} on the sensor AM1 is minimum while the others show significant change.

The $\log[(A_s-A_0)/(A_{max}-A_s)]$ was plotted versus log of the concentration of the respective metal ion to determine the binding constant and the stoichiometry of binding as reported[33]. This could not be done for AM1 as there was no significant change in its UV/Vis spectrum upon interaction with Hg^{2+}. Here, A_0 is the absorbance of the sensor before adding Hg^{2+} or Cu^{2+}, A_s is the absorbance at an intermediate concentration of added Hg or Cu, A_{max} is the absorbance of the sensor in presence of one equivalent Hg^{2+} or Cu^{2+}. The binding constant values and stoichiometric ratio obtained are quite similar to those obtained from the fluorescence data.

Determination of detection limit

The detection limits for the sensors towards Cu^{2+} and Hg^{2+} have been determined from fluorescence data by plotting (I_0-I_s) versus log of the respective metal ion concentration [33]. The results have been summarized in Table 1. The detection limits for different systems are found to be $10^{-5.5}$ M for AM1 sensing Hg^{2+}; $10^{-5.4}$ M for AM2 sensing Hg^{2+}; $10^{-5.0}$ M for AM3 sensing Cu^{2+} and $10^{-5.2}$ M for AM4 sensing Cu^{2+}.

Table 1
Analyte, Stoichiometry of analyte binding by the sensor, Binding constants and Detection Limits for different sensors.

Sensor	Analyte	Sensor:Analyte	Binding Constant	Detection Limit
AM1	Hg^{2+}	1:1	$10^{4.3}$ M	$10^{-5.5}$ M
AM2	Hg^{2+}	1:2	$10^{4.2}$ M	$10^{-5.4}$ M
AM3	Cu^{2+}	1:2	$10^{4.1}$ M	$10^{-5.0}$ M
AM4	Cu^{2+}	1:2	$10^{4.5}$ M	$10^{-5.2}$ M

DFT Calculations

Figure 5 shows the optimized geometries and shape of highest occupied molecular orbital (HOMO) of the molecules. The HOMO of all these molecules has contribution from the lone pair orbital of the nitrogen atom. Thus, these nitrogen atoms will be involved in the bond formation with the metal cations.

Fig. 6 shows the optimized geometries of the metal complexes of these molecules. All these metals are bonded to the ring nitrogen, oxygen atom of the carbonyl group as well as a weak interaction with the N-H moiety. The calculated binding energies of the each metal cation is significant (12.3 kcal/mol for AM1,

10.6 kcal/mol for AM2, 11.1 kcal/mol for AM3 and 9.6 kcal/mol for AM4) suggesting that the binding of these metal cations will be favorable.

Conclusions

The compounds derived from 4*H*-1,2,4-triazole-4-amine with benzoic acid and isophthalic acid could sense Hg^{2+} by fluorescence “on-off” mode with stoichiometry of binding 1:1 and 1:2 respectively. The binding constant and detection limits were $10^{4.3}$ and $10^{-5.5}$ M for the first sensor while these are $10^{4.2}$ and $10^{-5.4}$ M respectively. The compounds derived from 4*H*-1,2,4-triazole-4-amine with terephthalic acid and phthaleic acid could sense Cu^{2+} by fluorescence “on-off” mode. The binding constant and detection limits were $10^{4.5}$ and $10^{-5.0}$ M for the first sensor while these are $10^{4.2}$ and $10^{-5.2}$ M respectively. No interference was observed from other metal ions.

Declarations

Acknowledgement The authors thank DST for financial grant vide MRP (EMR/2016/001745) and FIST to the department. IIT-Kanpur is thanked for HRMS spectra.

Funding statement Funding received from DST, New Delhi (EMR/2016/001745).

Data availability statement Data sharing not applicable to this article as no datasets were generated or analysed during the current study.

Conflict of interest There are no conflict to declare.

Ethics approval Not applicable.

Consent to participate Not applicable.

Consent for publication Not applicable.

Author contribution : SD has done all the experiments works; AKG has done the computational works; DKD has done analysis of the results and written the paper.

References

[1] Z. Zhong, D. Zhang, D. Li, G. Zheng, Z. Tian, Tetrahedron (2016) Turn-on fluorescence sensor based on naphthalene anhydride for Hg2+ 72: 8050–8054.

[2] Z Zhu, Y Su, J Li, Di Li, J Zhang, S Song, Y Zhao, G Li, C Fan Anal. Chem. (2009) Highly Sensitive Electrochemical Sensor for Mercury(II) Ions by Using a Mercury-Specific Oligonucleotide Probe and Gold Nanoparticle-Based Amplification 81: 7660–7666.

[3] Z. Chen, T. Lou, Q. Wu, K. Li, L. Tan, J. Sun, Sens. Actuators B (2015) A facile label-free colorimetric sensor for Hg2+ based on Hg-triangular silver nanoplates with amalgam-like structure 221:365–369.

[4] M. Sarajli´, Z. Đuri´, V. Jovi´, S. Petrovi´, D. Dor – devi´, Microelectron. Eng. 2013 Detection limit for an adsorption-based mercury sensor 103: 118–122.

[5] K. Patir, S. K. Gogoi, Chem. Eng., 2018 Facile Synthesis of Photoluminescent Graphitic Carbon Nitride Quantum Dots for Hg2+ Detection and Room Temperature Phosphorescence 6: 1732–1743.

[6] T-bao Wei, G-ying Gao, W-juan Qu, B-bing Shi, Q Li, H Yao, Y-ming Zhang, Sens. Actuators B Chem. 2014 Selective fluorescent sensor for mercury(II) ion based on an easy to prepare double naphthalene Schiff base199: 142–147.

[7] M. Rex, F.E. Hernandez, A.D. Campiglia, Anal. Chem. (2006) Pushing the Limits of Mercury Sensors with Gold Nanorods 78: 445–451.

[8] W. Shi, H. Ma, Chem. Commun. 2008 Rhodamine B thiolactone: a simple chemosensor for Hg2+ in aqueous media 16: 1856–1858.

[9] W. Lin, X. Cao, Y. Ding, L. Yuan, L. Long, Chem. Commun. 2010 A highly selective and sensitive fluorescent probe for Hg^{2+} imaging in live cells based on a rhodamine–thioamide– alkyne scaffold 46: 3529–3531.

[10] X.Q. Chen, T. Pradhan, F. Wang, J.S. Kim, J. Yoon, Chem. Rev. 2012 Fluorescent chemosensors based on spiroring-opening of xanthenes and related derivatives 112: 1910–1916.

[11] M.G. Choi, Y.H. Kim, J.E. Namgoong, S.K. Chang, Chem. Commun. (2009) Hg^{2+} -selective chromogenic and fluorogenic chemodosimeter based on thiocoumarins 24: 3560–3562.

[12] J.E. Namgoong, H.L. Jeon, Y.H. Kim, M.G. Choi, S.K. Chang, Tetrahedron Lett. (2010) Hg^{2+} -selective fluorogenic chemodosimeter based on naphthoflavone 51: 167–169.

[13] W. Jiang, W. Wang, Chem. Commun. (2009) A selective and sensitive “turn-on” fluorescent chemodosimeter for Hg2+ in aqueous media via Hg^{2+} promoted facile desulfurization–lactonization reaction 29: 3913–3915.

[14] S. Winch, T. Praharaj, D. Fortin, D.R. Lean, Sci. Total Environ. (2008) Factors affecting methylmercury distribution in surficial, acidic, base-metal mine tailings 392 (2008) 242–251.

[15] A. K. Shigemoto, C. N. Virca, S. J. Underwood, L. R. Shetterly, T. M. Mccormick. J. Coord. Chem. 69 (2016) 2081–2089.

[16] K. Bera, A. K. Das, M. Nag, S. Basak, Anal. Chem. (2014) Thiophene-based fluorescent mercury-sensors 86: 2740–2746.

[17] H. Ju, D. J. Chang, S. Kim, H. Ryu, E. Lee, In-Hyeok Park, J. H. Jung, M. Ikeda, Y. Habata, S. S. Lee. Inorg. Chem. (2016) Cation-Selective and Anion-Controlled Fluorogenic Behaviors of a Benzothiazole-Attached Macrocycle That Correlate with Structural Coordination Modes 55: 7448–7456.

[18] Tai-bao Wei, Guo-ying Gao, Wen-juan Qu, Bing-bing Shi, Qi Lin, Hong Yao, You-ming Chang. Sensors and Actuators B (2014) Selective fluorescent sensor for mercury(II) ion based on an easy to prepare double naphthalene Schiff base 199: 142–147.

[19] D Udhayakumari, S. Velmathi, Supramolecular Chem., (2015) Naphthalene thiourea derivative based colorimetric and fluorescent dual chemosensor for F− and Cu2+/Hg2+ ions 27: 539–544.

[20] Qi-Yin Chena, Chuan-Feng Chen, Tetrahedron Letters, (2005) A new Hg2+-selective fluorescent sensor based on a dansyl amide-armed calix[4]-aza-crown 46:165–168.

[21] S. Das, A. Sarkar, A. Rakshit, A. Datta, Inorg. Chem. (2018) A Sensitive Water-Soluble Reversible Optical Probe for Hg2+ Detection 57: 5273–5281.

[22] E. L. Que, D. W. Domaille, C. J. Chang, Chem. Rev., 108 (2008) 1517–1549.

[23] B. Sarkar, Chem. Rev., 99 (1999) 2535–2544.

[24] Y. K. Jang, U. C. Nam, H. L. Kwon, I. H. Hwang, C. Kim, Dyes Pigm., (2013) A selective colorimetric and fluorescent chemosensor based-on naphthol for detection of Al^{3+} and Cu^{2+} 99: 6–13.

[25] X. Zhang, M. Kang, H. Choi, J. Y. Jung, K. M. K. Swamy, S. Kim, D. Kim, J. Kim, C. Lee, J. Yoon, Sens. Actuators, B, (2014) Organic radical-induced Cu^{2+} selective sensing based on thiazolothiazole derivatives 192: 691–696.

[26] B. Schleper, H. J. Stuerenburg, J. Neurol., (2001) Copper deficiency-associated myelopathy in a 46-year-old woman. 248:705–706.

[27] X. Yang, W. Zhang, Z. Yi, H. Xu, J. Wei, L. Hao, New J. Chem., (2017) Highly sensitive and selective fluorescent sensor for copper(II) based on salicylaldehyde Schiff-base derivatives with aggregation induced emission and mechanoluminescence 41:11079.

[28] J. Kumar, P.K. Bhattacharyya, D.K. Das, Spectrochim. Acta A, (2015) New duel fluorescent “on–off” and colorimetric sensor for Copper(II): Copper(II) binds through N coordination and pi cation interaction to sensor 138: 99.

[29] Y. Zhao, D. G. Truhlar, Theor. Chem. Acc. (2008) The M06 suite of density functional for main group thermochemistry, thermochemical kinetics, noncovalent interactions, excited states, and transition elements: two new functionals and systematic testing of fourM06-class functional and 12 other functionals. 120:215.

[30] a) A. E. Reed, F. Weinhold, J. Chem. Phys. (1983) Natural bond orbital analysis of near -Hartree-Fock water dimer 788:4066; b) A. E. Reed, R. B. Weinstock, F. Weinhold, J. Chem. Phys. 83 (1985) Natural population analysis 83:735; c) A. E. Reed, L. A. Curtiss, F. Weinhold, Chem. Rev. (1988) Intermolecular interactions from a natural bond orbital, donor acceptor view point 88:899.

[31] M. J. Frisch et. al. *Gaussian 16 (Revision A.03)*, Gaussian, Inc., Wallingford CT, (2016).

[32] B. Bharali, S. Goyari, D K Das, J Fluorescence (2018) Condensation Product of 4-Methoxybenzaldehyde and Ethylenediamine: “Off-On” Fluorescent Sensor for Cerium(III) 28:1357-1361.

[33] D.K. Das, S. Deka, A.K. Guha, J Fluoresce. (2019) Schiff Base Derived from 4,4'-methylenedianiline and p-anisaldehyde: Colorimetric Sensor for Cu^{2+}, Paper Strip Sensor for Al^{3+} and Fluorescent Sensor for Pb^{2+} 29:1467–1474.

Figures

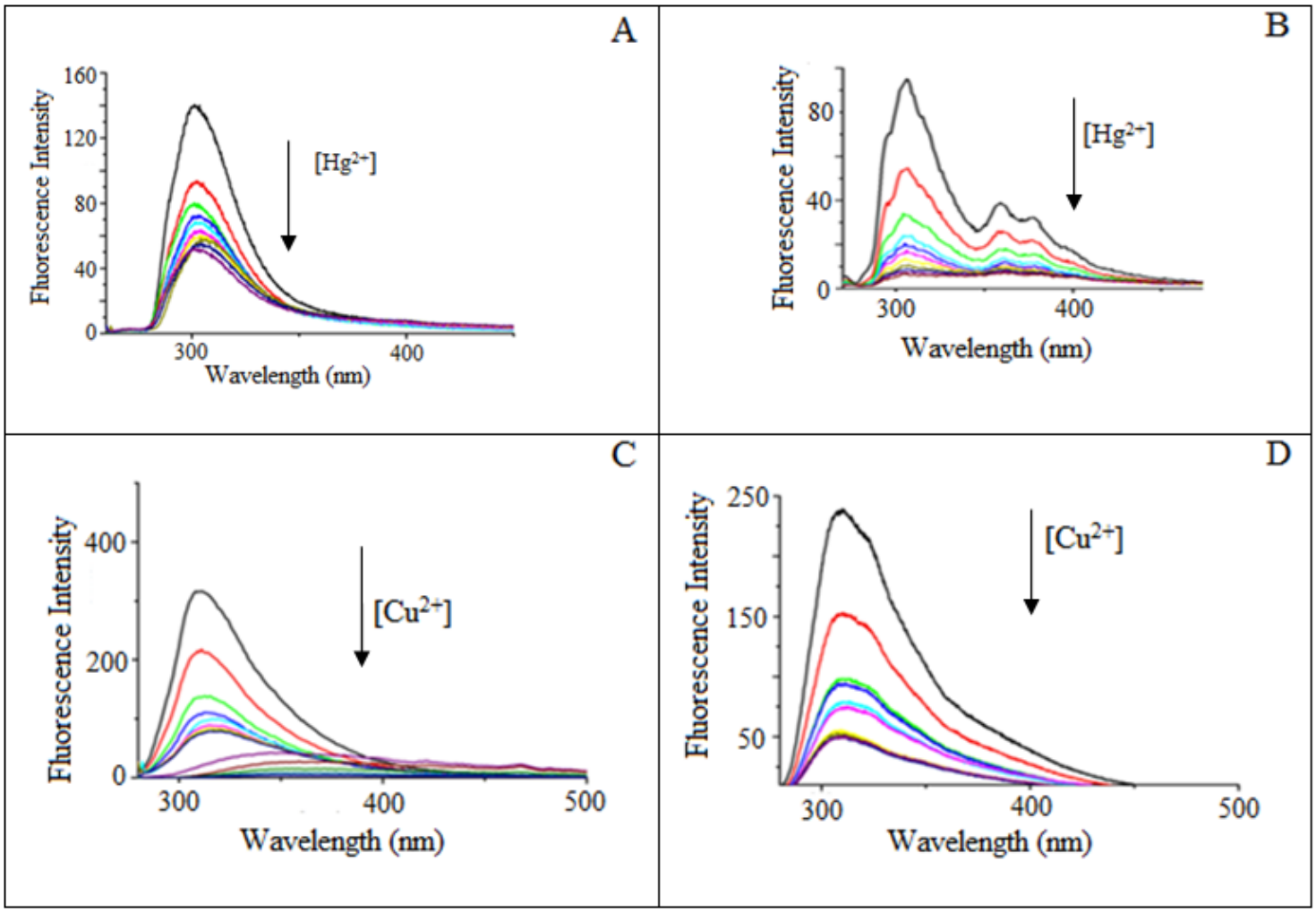

Figure 1

Effect of Hg2+ on fluorescence spectrum of AM1 (A) and AM2 (B); effect of Cu2+ on fluorescence spectrum of AM3 (C) and AM4 (D) in 1:1 v/v CH3:H2O

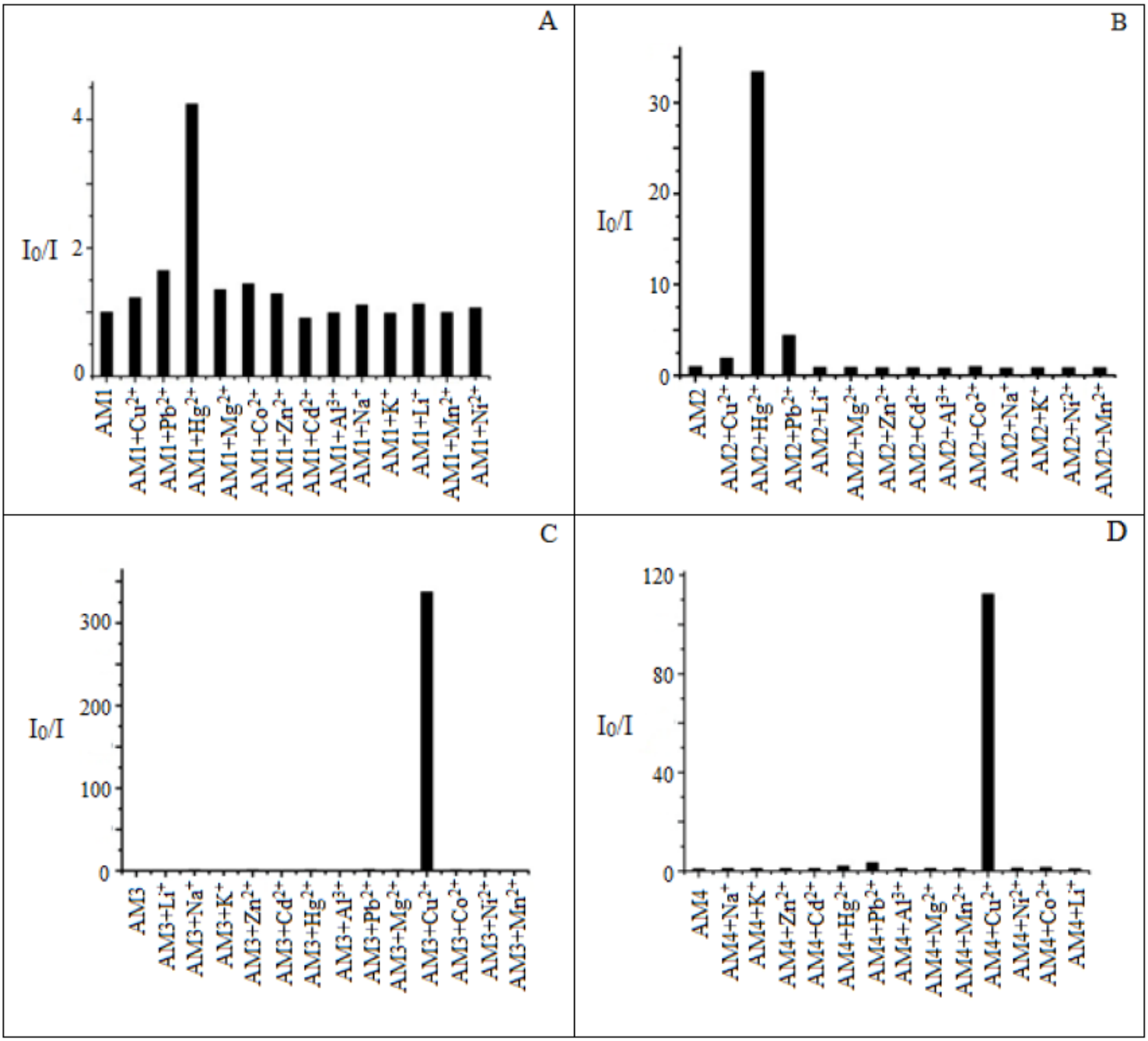

Figure 2

Bar diagrams for I0/I values of AM1 (A), AM2 (B), AM3 (C) and AM4 (D) in presence of different metal ions in 1:1 v/v CH3:H2O.

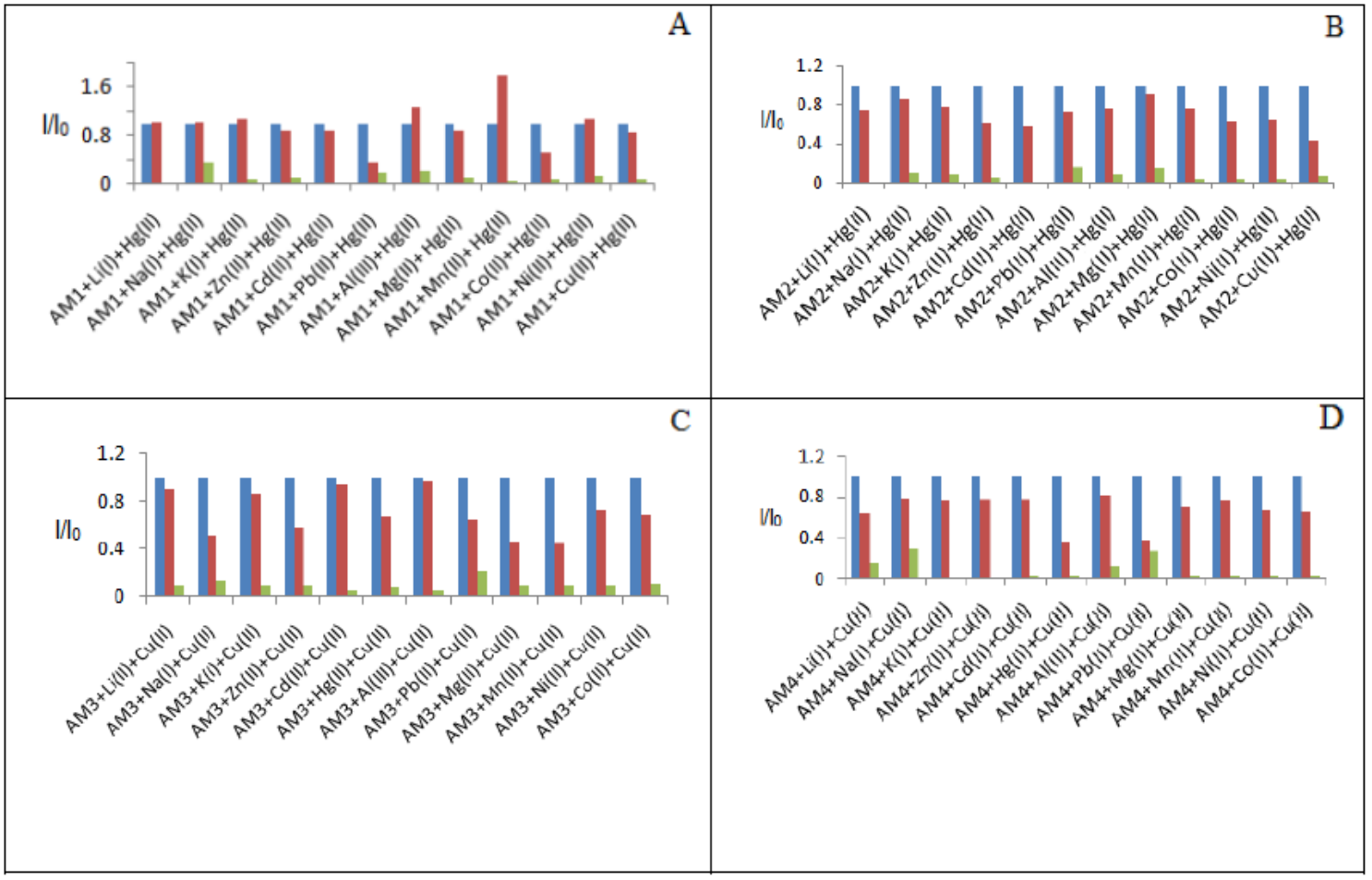

Figure 3

I/I0 response of – (A) AM1(blue bars), AM1+Mn+ (red bars), AM1+Mn++Hg2+ (green bars); (B) AM2 (blue bars), AM2+Mn+ (red bars), AM2+Mn++Hg2+ (green bars) (C) AM3 (blue bars), AM3+Mn+ (red bars), AM3+Mn++Cu2+ (green bars); (D) AM4 (blue bars), AM4+Mn+ (red bars), AM4+Mn++Hg2+ (green bars) in 1:1 (v/v) CH3OH:H2O. Mn+ is Li+, Na+, K+, Zn2+, Al3+, Mg2+, Mn2+, Co2+, Ni2+, Cu2+, Cd2+, Pb2+ and Hg2+.

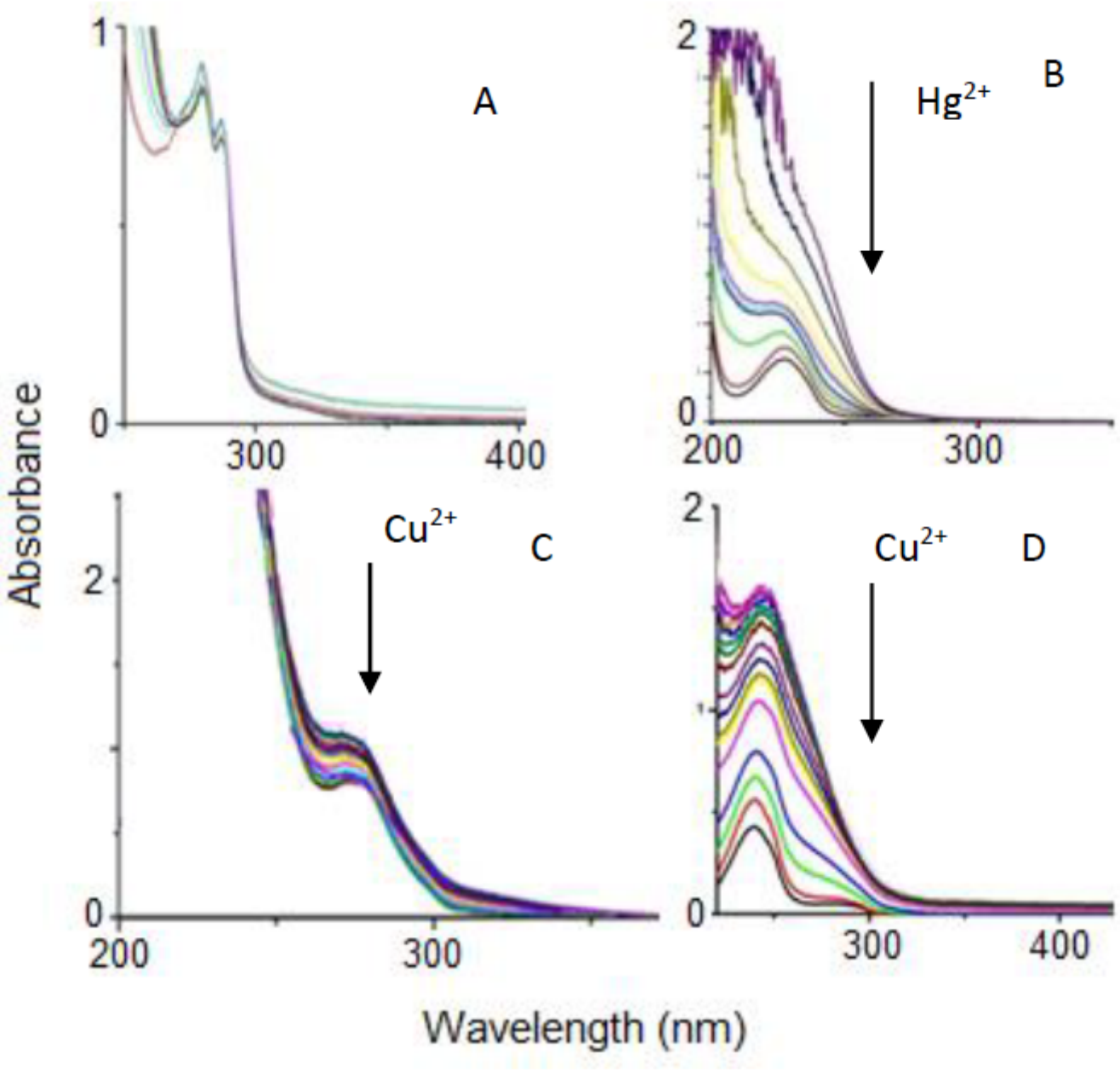

Figure 4

UV/Visible spectra of – (A) AM1 and (B) AM2 at different added concentration of Hg2+; (C) AM3 and (D) AM4 at different added concentration of Cu2+ in 1:1 (v/v) CH3OH:H2O.

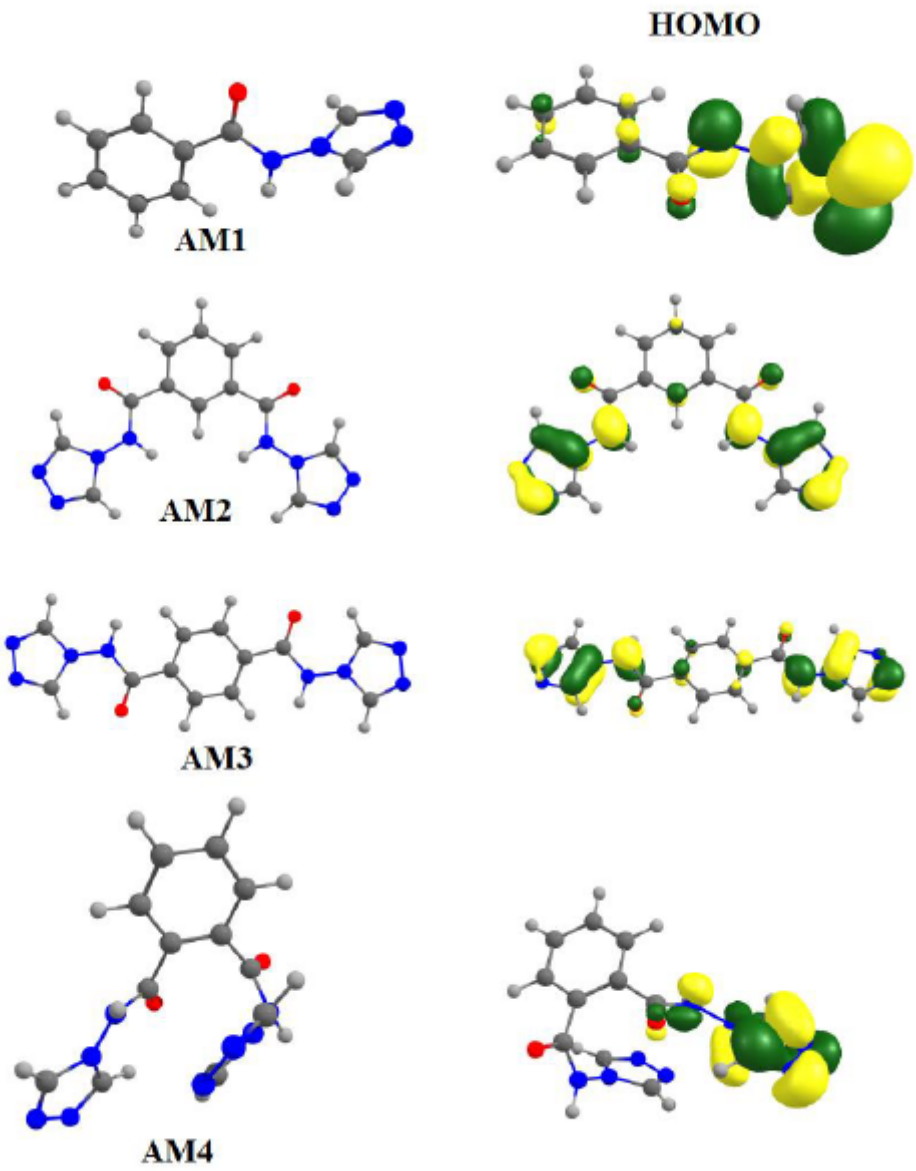

Figure 5

Optimized geometries of the molecules along with the shape of HOMO with a contour value of 0.03 a.u.

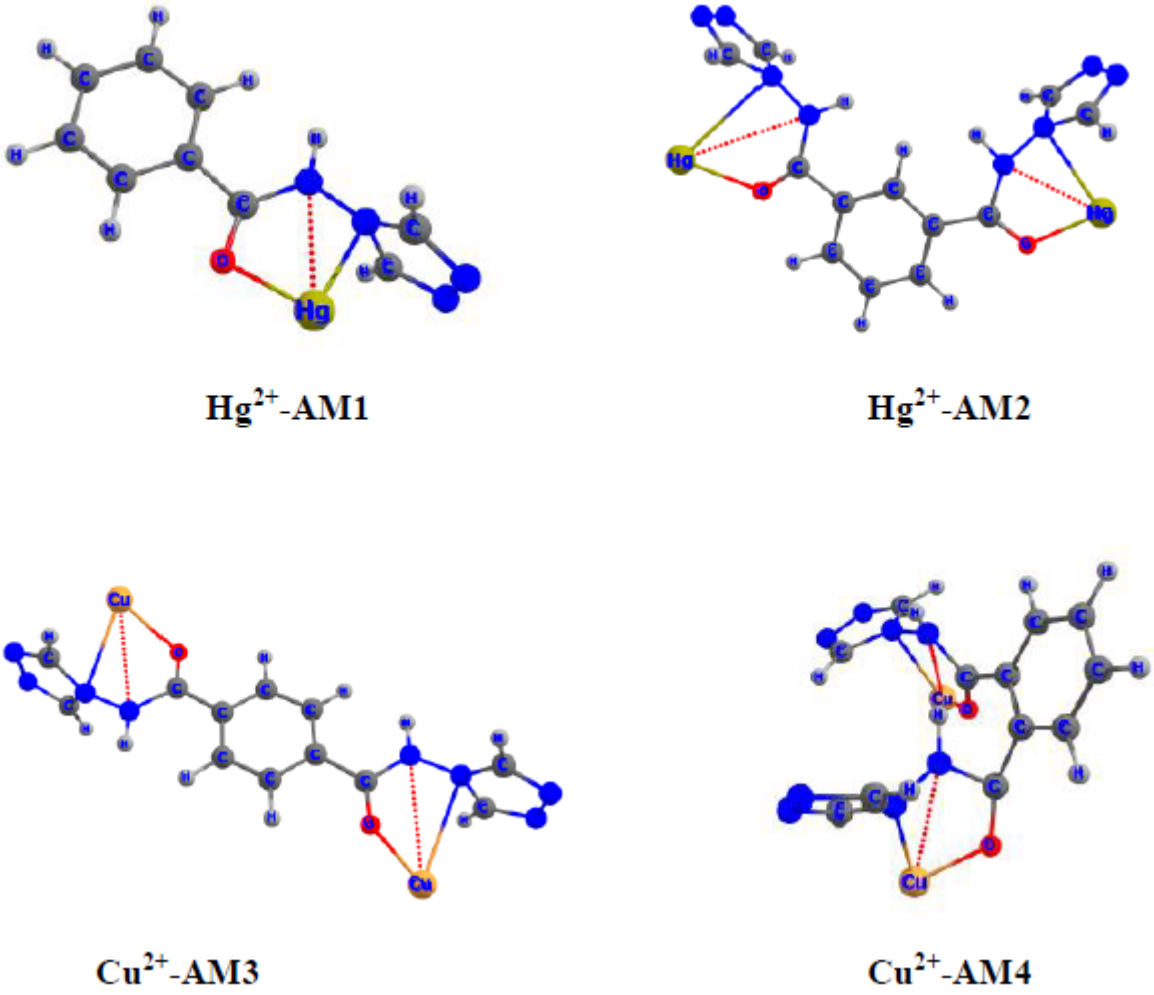

Figure 6

Optimized geometries of the metal complexes.

Supplementary Files

This is a list of supplementary files associated with this preprint. Click to download.

- Scheme1.png
- Scheme2.png